Cardiology in the Young (2016), **26**, 1543–1552
doi:10.1017/S1047951116001219

Review Article

Assessment of the structure and function of the aorta by echocardiography

Anitha Parthiban, Girish Shirali

Ward Family Heart Center, Children's Mercy Hospital, Kansas City, Missouri, United States of America

Abstract Echocardiography is the primary modality for imaging the aorta for the diagnosis and serial evaluation of pathological conditions. In this article, we review the methodology for optimal echocardiographic imaging of the various segments of the aorta and discuss abnormalities of the aorta including stenosis, dilation including aortopathy and sinus of Valsalva aneurysms, and fistulous communications involving the ascending aorta including aortoventricular tunnel and ruptured sinus of Valsalva aneurysm. We review novel echocardiographic measurements of aortic functional properties of the aorta such as elasticity and stiffness, and review the literature on the potential additive value of such measurements for structural assessment alone. Finally, we discuss the limitations of echocardiography in the precise and optimal imaging of the aorta.

Keywords: Supravalvar aortic stenosis; sinus of Valsalva aneurysm; aortoventricular tunnel; echocardiographic imaging of the aorta; aortic stiffness

Received: 20 May 2016; Accepted: 3 July 2016

THE AORTA IS THE LARGEST ARTERY IN THE BODY; it functions as a pulsatile and elastic conduit carrying stroke volume from the left ventricle to the systemic circulation. Pathological conditions of the aorta vary in their clinical presentation with regard to age, clinical features, and severity; these variations may be particularly pronounced in childhood. Echocardiography remains the first-line modality of imaging in children because of ease of access, safety, and acceptable image quality, and it is the most commonly used test to diagnose and to serially monitor the structure and function of the aorta. As absolute measurements or trends in serial measurements of the aorta over time are used to make decisions pertaining to management, such as pharmacological therapy or surgical replacement of the aorta, it is critical that a standardised approach be used within and across echocardiographic laboratories to make such measurements.

Correspondence to: A. Parthiban, MD, Children's Mercy Hospital, 2401 Gillham Road, Kansas City, MO 64108, United States of America. Tel: +816 234 3255; Fax: 816 302 9987; E-mail: aparthiban@cmh.edu

Echocardiographic evaluation of the aorta

The aorta begins as a bulb-shaped root distal to the aortic valve. It courses cranially before arching in a candy-cane configuration to then extend caudally through the thorax and abdomen before its termination at the iliac bifurcation.[1] It consists of five anatomical segments; from the proximal to distal ends these are the aortic root, ascending aorta, aortic arch, descending thoracic aorta, and descending abdominal aorta. The aortic root includes the aortic valve annulus, sinuses of Valsalva, and the coronary ostia. The sinotubular junction demarcates the aortic root from the ascending aorta, which extends to the brachiocephalic artery. The aortic arch extends from the brachiocephalic artery to the left subclavian artery; the descending thoracic aorta extends from the left subclavian artery to the diaphragm, and the descending abdominal aorta extends from the diaphragm to the iliac bifurcation. The retrosternal position of the ascending aorta, the complex geometry of the aortic arch, and its close anatomic relationship with the airway are all factors that may

contribute to the difficulty in imaging the aorta by echocardiography, especially in patients of larger size. Standard echocardiographic evaluation of the aorta should include two-dimensional, color Doppler, and pulsed wave Doppler interrogation from various windows and imaging planes in order to optimally visualise the maximal extent of the aorta.

How and where to make measurements of the aorta by transthoracic echocardiography?

In 2010, guidelines for making standardised measurements of the various segments of the aorta in the paediatric age group were published.[2] Normal reference values adjusted for age and body size are available.[3,4] In children, the guidelines recommend to obtain the measurements in mid systole, at maximal expansion, and between the inner edges of the opposing walls. This differs from adult guidelines, which recommend obtaining the measurements in diastole, between leading edges.[1] In general, care must be taken to align the transducer such that the measurements are made in the long axis of the vessel; oblique alignment should be avoided to avoid errors and to ensure reproducibility. The image should focus on the region of interest in order to optimise spatial and temporal resolution. In addition, optimal positioning of the patient – left/right lateral decubitus for the respective high parasternal views and the use of a roll behind the shoulders with extension of the neck for the suprasternal notch view – is critical to obtain images of good quality.

Measurements of the proximal aorta should include the aortic root at the sinuses of Valsalva, sinotubular junction, and the ascending aorta at the level of the right pulmonary artery. Moving the transducer one to two intercostal spaces superior to the traditional parasternal window or the high right parasternal window allows for improved visualisation of the ascending aorta. Measurements of the proximal transverse arch (between the two carotid arteries), distal transverse arch (between the left carotid and left subclavian arteries), and the aortic isthmus (narrowest diameter distal to the left subclavian artery), are best obtained in the suprasternal long-axis view of the aortic arch. The descending aorta diameter is measured at the level of the diaphragm from the subxiphoid views. Pulsed wave Doppler evaluation of the aorta is useful to identify and quantify obstruction if present. Doppler interrogation is best performed from the apical or the right parasternal views for the proximal aorta, suprasternal short- or long-axis view for the ascending aorta, suprasternal long-axis view for the aortic arch, and subxiphoid long-axis view for the abdominal aorta. The techniques to image and measure the various segments of the aorta by transthoracic echocardiography are depicted in Figure 1a–d.

In addition, three-dimensional echocardiography has been useful in evaluating disorders of the aorta such as aneurysms of the sinus of Valsalva and aorto-ventricular tunnel.[5–7] In our experience, the use of *X*-plane and scan angle functions has been useful to obtain orthogonal views of various structures such that diameters could be obtained in two planes (Fig 2/Supplementary video 1).

Supravalvar aortic stenosis

Supravalvar aortic stenosis is characterised by narrowing of the aorta that typically extends cranial to the superior margin of the sinuses of Valsalva. It may occur as a part of syndromes such as Williams–Beuren syndrome or as a familial autosomal dominant condition; in some cases, it may be sporadic. From the histopathological standpoint, the arteriopathy affects elastin involving the proximal aorta to a variable extent.[8] Morphological types described include hourglass narrowing of the sinotubular junction, diffuse tubular narrowing of the ascending aorta, or a discrete shelf-like membrane causing obstruction to blood flow (Fig 3a/Supplementary video 2). The aortic valve leaflets are thickened in 50% of the cases with restricted mobility due to tethering at the stenotic sinotubular junction. In about 30% of the patients, there is diffuse stenosis of the entire ascending aorta that extends to the brachiocephalic vessels.[9] With the Williams–Beuren syndrome, coronary artery abnormalities such as enlargement of the proximal coronary arteries due to the high-pressure conditions proximal to the supravalvar narrowing, ostial stenosis due to the extension of the intimal hyperplasia into the coronary ostia, or ostial atresia can occur. Stenosis of the peripheral pulmonary arteries is commonly an associated feature.

Supravalvar aortic stenosis is best imaged in the parasternal long-axis view as either an hourglass-type narrowing at the sinotubular junction or a diffuse tubular hypoplasia of the ascending aorta that may extend to the innominate artery. There is intimal hyperplasia with resulting echo brightness of the walls of the affected segment of the aorta. The extent of the narrowing in the aorta should be delineated by using the views mentioned in the previous section. Aortic valve function must be assessed by two-dimensional and Doppler echocardiography from apical and parasternal views. The proximal coronary arteries should be carefully evaluated in the parasternal short-axis views for ostial stenosis or enlargement. The brachiocephalic vessels should be evaluated by two-dimensional and color flow Doppler for evidence of stenosis; post-stenotic dilation of the innominate artery may also occur.

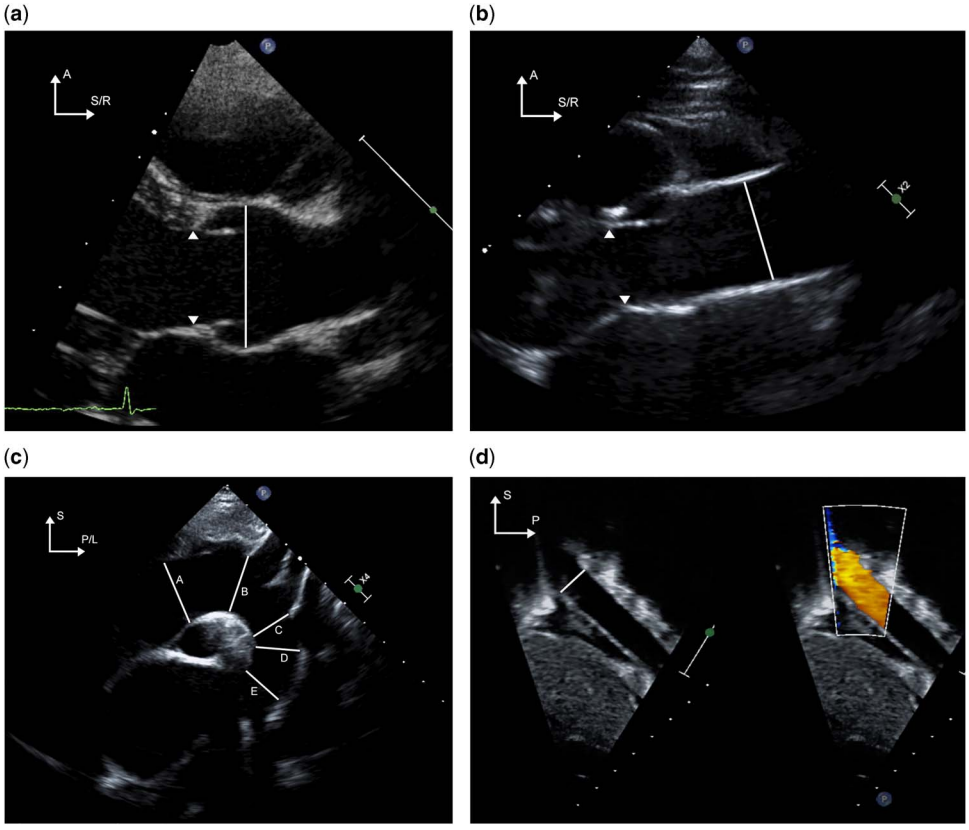

Figure 1.
*The techniques for imaging the various sections of the aorta from various echocardiographic windows are demonstrated. (**a**) The aortic valve and root are imaged from the parasternal long-axis window. The arrowheads indicate the hinge points of the aortic valve. The diameter of the aortic root is measured in systole from inner edge to inner edge as shown by the solid line. By moving one to two intercostal spaces higher than the traditional parasternal window, the ascending aorta is imaged in its long axis (**b**); care must be taken to avoid angulated insonation. The solid line indicates the diameter of the ascending aorta; the arrowheads point to the hinges of the aortic valve. Imaging from the suprasternal notch (**c**) allows for visualisation of the aortic arch including the distal ascending aorta (**A**), proximal transverse arch (**B**), distal transverse arch (**C**), aortic isthmus (**D**) and proximal descending thoracic aorta (**E**). In panel (**d**), the descending abdominal aorta is imaged at and inferior to the level of the diaphragm from the subcostal sagittal plane. The solid line represents the diameter of the descending aorta at the level of the diaphragm. A = anterior; L = left; P = posterior; R = right; S = superior.*

The retrosternal position of the ascending aorta may prevent adequate visualisation of the entire extent of supraaortic stenosis. Evaluation of the pressure gradient in supravalvar stenosis by pulsed wave Doppler is challenging for several additional reasons. Owing to the orientation of the stenotic orifice, the flow jet may be eccentric and difficult to sample accurately. Overestimation or underestimation of gradients by Doppler can occur if there are multiple areas of obstruction or long-segment stenosis, and it may be difficult to isolate these from gradients arising from other structures such as the branch pulmonary arteries. As the jet of flow is often directed towards the brachiocephalic artery, Doppler interrogation from the suprasternal notch view often yields the highest gradients (Fig 3b). Concentric left ventricular hypertrophy is an indirect indicator that significant stenosis may be present.

Aneurysms of the Sinus of Valsalva

Aneurysms of the sinus of Valsalva are characterised by dilation of one or more of the sinuses of Valsalva. Patients with this lesion are frequently asymptomatic until the rapid haemodynamic compromise that results from the sudden rupture of aneurysms; consequently, they present infrequently in childhood, although they have been reported in the literature.[10–13] They may be congenital or occur as a complication of diseases such as Marfan syndrome or endocarditis. Over half occur in association with ventricular septal defects, but they may present as isolated lesions;[14] association with other CHD has also been described.[15–17] Echocardiography allows the diagnosis of these lesions with a high degree of sensitivity and specificity.[14] A sinus of Valsalva aneurysm is typically seen as a thin saccular structure

https://doi.org/10.1017/S1047951116001219 Published online by Cambridge University Press

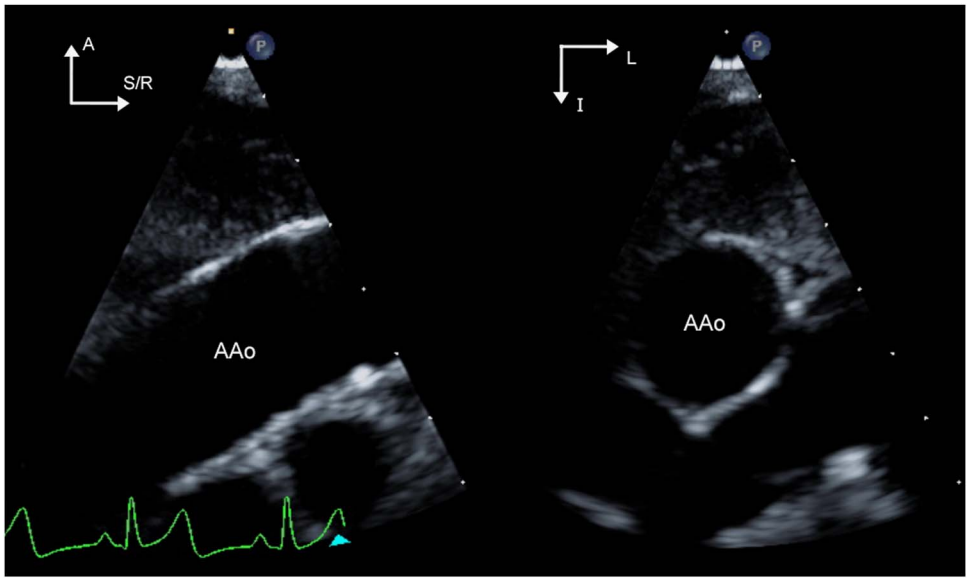

Figure 2.
(Supplementary video 1) X-plane imaging of the ascending aorta (AAo) is demonstrated. The image on the left shows a zoomed view of the ascending aorta imaged from the high parasternal window. By applying X plane, the orthogonal view is obtained (image on right). Note the change in orientation as indicated by the arrows in the top left-hand corner of each image. The right-sided image is obtained by electronic clockwise rotation of the left-sided image by 90°. This allows for making measurements of a given structure in orthogonal planes. The plane of interrogation of the right-sided image can be adjusted in live imaging by manipulation of the trackball. In this case, the plane of interrogation is indicated by the white arrowhead seen at the bottom of the left-sided image. A = anterior; I = inferior; L = left; R = right; S = superior.

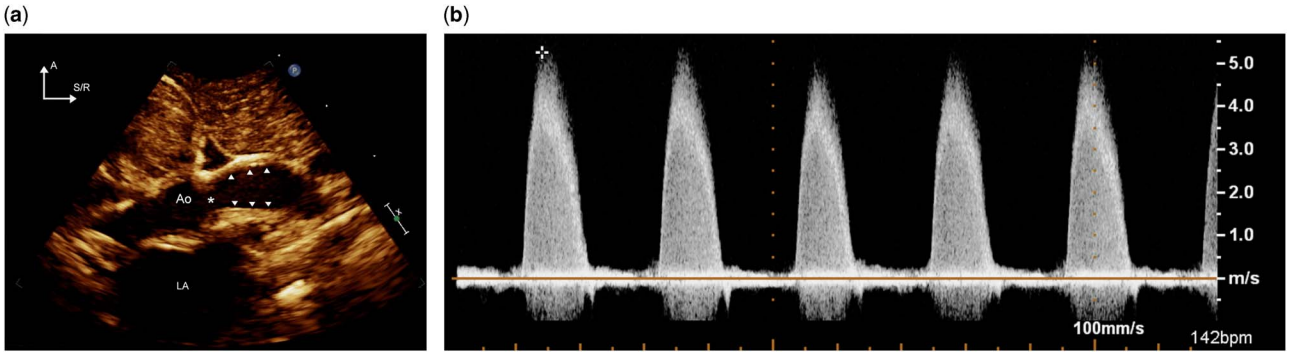

Figure 3.
*(Supplementary video 2) Panel (**a**) shows the high parasternal long-axis image of the ascending aorta (Ao) in a patient with supravalvar aortic stenosis; note the hourglass-shaped narrowing at the sinotubular junction of the aorta indicated by the asterisk. In addition, extending distal to the sinotubular junction, there is thickening and echo brightness of the walls of the ascending aorta, which is shown by the arrowheads. Continuous wave Doppler interrogation of the ascending aorta from the suprasternal notch is shown in (**b**); the peak gradient is >100 mmHg. Care must be taken to orient the transducer such that the Doppler beam is aligned to be parallel to the jet of prograde flow in order to avoid underestimation of the gradient. A = anterior; LA = left atrium; R = right; S = superior.*

arising from the aortic sinus just superior to the aortic valve annulus. The majority of these arise from the right coronary sinus (>75%) followed by the non-coronary and left coronary sinuses; multiple aneurysms have also been reported.[11,13] The aneurysms most frequently expand and protrude into the right atrium or ventricle (Fig 4a/Supplementary video 3), although expansion into the interatrial and interventricular septae, ventricular free wall, and extracardiac expansion can occur. The origin and extent of the aneurysm can be defined from the parasternal views using two-dimensional echocardiography. Echocardiographic evaluation should also include assessment for the haemodynamic effects of the aneurysm, which, in the unruptured state, include aortic/tricuspid valve regurgitation, outflow tract obstruction due to space-occupying effect, thrombosis, coronary occlusion, and conduction disturbances. When sinus of Valsalva aneurysms present with rupture, color and pulsed wave Doppler evaluations

https://doi.org/10.1017/S1047951116001219 Published online by Cambridge University Press

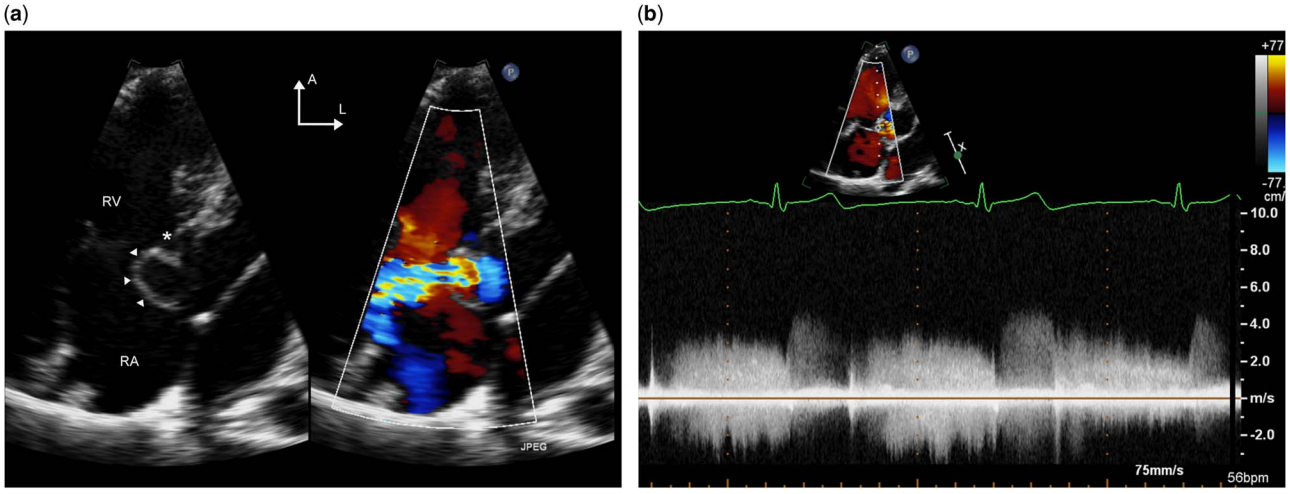

Figure 4.
*(Supplementary video 3) Panel (**a**) depicts the parasternal short-axis view from a patient with aneurysm of the sinus of Valsalva. The aneurysm is visualised as a thin-walled saccular structure protruding into the right atrium (RA) and is shown by the arrowheads. The asterisk shows the hinge point of the septal leaflet of the tricuspid valve. The aneurysm has ruptured into the RA (blue jet). Panel (**b**) shows the continuous high-velocity signal that was obtained using continuous wave Doppler interrogation of the jet. This helps in differentiating this lesion from a ventricular septal defect with aortic valve prolapse and aortic insufficiency, in which case there would be two separate high-velocity jets: one due to systolic flow from the ventricular septal defect, and the other due to high-velocity diastolic flow from the aortic insufficiency. Images are courtesy of Geoffrey Forbus, MD, Medical University of South Carolina, Charleston, South Carolina, United States of America. A = anterior; L = left; RV = right ventricle.*

reveal a high-velocity continuous left-to-right shunt, in the case of rupture into the right ventricle (most common), right atrium, left atrium, or pulmonary artery, whereas rupture into the left ventricle results in diastolic flow similar to aortic regurgitation (Fig 4b). Typically, the thoracic aorta is enlarged and significant diastolic flow reversal can be demonstrated by color flow and spectral Doppler. Aneurysms that expand into the extracardiac space rupture into the pericardial or pleural space and can be rapidly fatal. Transoesophageal echocardiography can be useful as a complementary technique for delineation of the aneurysm and the site of rupture.

Ruptured aneurysms of the sinus of Valsalva must be distinguished from ventricular septal defects with prolapse of the aortic valve with aortic regurgitation, and from aortoventricular tunnel, because the timing of intervention varies dramatically among these diagnoses. The position of the aortic end of the defect with respect to the coronary ostia and the aortic valve annulus are helpful in this regard. The aortic end of a sinus of Valsalva aneurysm is above the hinges of the aortic valve leaflets and typically below the coronary ostia. In contrast, with a ventricular septal defect with prolapse of the aortic valve, the involved aortic cusp is distorted and elongated and extends into the ventricle inferior to the aortic valve annulus. In a left ventricle-to-aorta tunnel, the aortic end of the defect is typically superior to the coronary ostia. Furthermore, tunnels usually have a longer course than ruptured aneurysms.

Although the difference between the aneurysm of sinus of Valsalva and left ventricle-to-aorta tunnel is readily apparent to the surgeon or pathologist in that the latter structure is visible on inspection of the external surface of the heart, the differential diagnosis by echocardiography can be challenging. Careful sweeps of the proximal aorta extending to the base of the heart need to be performed to understand the orientation of the defect with respect to the coronary ostia and the aortic valve annulus.

Aortoventricular tunnel

Aortoventricular tunnel is a rare entity. It consists of a channel that connects the ascending aorta to the ventricular chamber resulting in diastolic run-off from the aorta. Most forms of these tunnels communicate with the left ventricle, although they may communicate with the right atrium or right ventricle.[6,18–20] In aorto–left ventricular tunnel, the aortic end of the tunnel is typically situated in the anterior aortic wall superior to the ostium of the right coronary artery. The ventricular end of the tunnel is situated in the triangular area between the right and left coronary leaflets of the aortic valve and it is the deficiency of this wall and resulting "unhinging" of the right coronary leaflet that is hypothesised to be the aetiology of this unusual defect. There can be aneurysmal dilation of any or all portions of the tunnel; dilation of the intracardiac portion that

https://doi.org/10.1017/S1047951116001219 Published online by Cambridge University Press

courses between the aortic sinus and the subpulmonary infundibulum may result in right ventricular outflow obstruction. Aortic valve stenosis and even atresia have been described in association with this condition. The condition should be suspected in the fetus or infant with severe aortic insufficiency and congestive heart failure.

In addition to being rare, potential misdiagnosis as ventricular septal defects or aortic valve disease can make the diagnosis by echocardiography challenging.[21] On two-dimensional echocardiography, there is evidence for hypertrophy and volume overload of the left ventricle. Aneurysmal thinning of the ventricular septum has been described.[7] In the parasternal and apical long-axis sweeps, the tunnel can be identified as a structure coursing between the aorta and the right ventricular outflow tract and providing an additional source of egress to blood flow from the left ventricle in addition to the more posterior left ventricular outflow tract (Fig 5a and b, Supplementary videos 4 and 5).

Spectral and color Doppler flow show aortic regurgitation occurring through the tunnel (Fig 5c). The aortic end of the aorto–left ventricular tunnel may be confused for a ventricular septal defect; however, the flow is diastolic, and on careful inspection the communication with the aorta – rather than the right ventricle – can be identified. The ascending

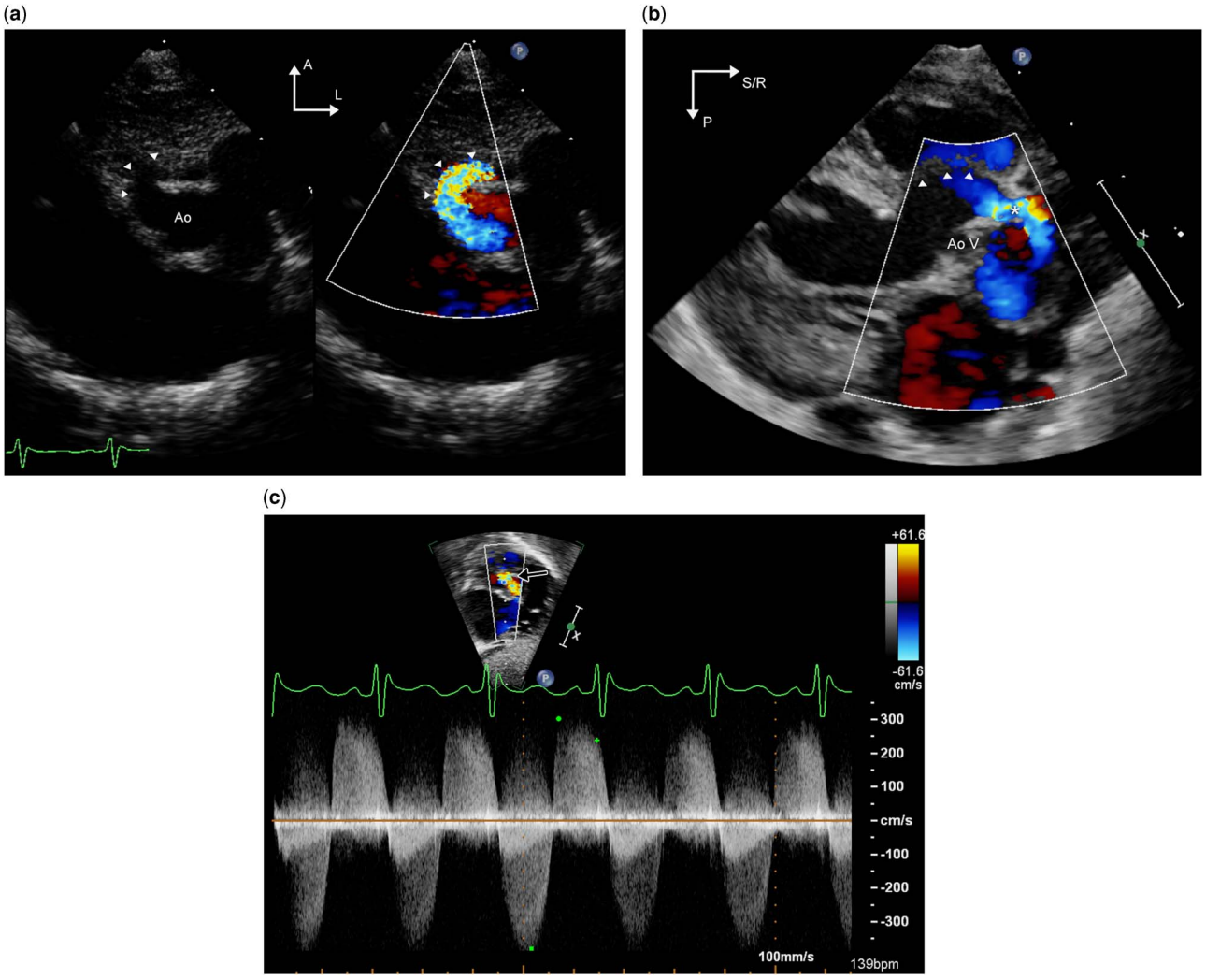

Figure 5.
*Transthoracic echocardiographic images from a patient with left ventricle–aorta tunnel. Panel (a)/Supplementary video 4 is a parasternal short-axis image that shows the tunnel (arrowheads) coursing anterior to the aorta. Panel (**b**)/Supplementary video 5 is a parasternal long-axis image from the same patient. The interventricular septum, which is indicated by the arrowheads, is thinned out and aneurysmal. The aortic valve is thickened and does not open in systole. There is to and fro flow through the tunnel, depicted by the asterisk, anterior to the aortic valve annulus. Panel (**c**) is a subcostal long-axis view that depicts continuous wave Doppler interrogation of the tunnel (black arrow); this exhibits high-velocity bidirectional flow in both systole and diastole. This may be confused with aortic valve disease with combined aortic stenosis and regurgitation. A = anterior; Ao = aorta; AoV = aortic valve; L = left; P = posterior; R = right; S = superior.*

https://doi.org/10.1017/S1047951116001219 Published online by Cambridge University Press

aorta is typically dilated and there is color and pulsed wave Doppler evidence of diastolic run-off in the aortic arch and descending aorta. In the parasternal short-axis view, the tunnel is seen as a dilated structure anterior to the aortic valve, and encroachment into the right ventricular outflow tract may be evident. By angling the transducer superiorly from the parasternal short-axis view or from the high parasternal views, the ostium of the right coronary artery is identified and the spatial relationship and proximity of the ostium to the aortic end of the tunnel should be determined. These sweeps are helpful in differentiating this lesion from ruptured sinus of Valsalva aneurysms and have implications for surgical planning. It is important to remember that Doppler assessment of the aortic valve may not be an accurate method to assess the severity of aortic valve stenosis in the presence of low-resistance egress to blood flow provided by the tunnel; two-dimensional assessment of the valve is of much greater value.

Aorto–right ventricular tunnel is even rarer with only isolated case reports in the literature; it is similar to the aorto–left ventricular tunnel except that the ventricular end of the tunnel is in the right ventricle.[6,22,23] The right ventricle is pressure and volume overloaded from the shunt and is typically hypertrophied and enlarged. In contrast to communications with the left ventricle, aortic valve abnormalities are not commonly associated but pulmonary stenosis has been described.[24,25] In the setting of critical pulmonary stenosis, the tunnel may be misdiagnosed as a ventriculocoronary communication. The absence of coronary artery dilation is helpful in differentiating the tunnel from ventriculocoronary fistulous communications.

Aortopathy

Aortopathy is defined as pathological dilation of the aorta; this may result in aneurysm formation and predispose to death from rupture or dissection. A number of disease entities – both syndromic such as Marfan, Loeys–Dietz, Ehlers–Danlos, and Turner syndrome and sporadic, such as bicuspid aortic valve-associated aortopathy and familial thoracic aneurysm syndromes – can result in aortopathy.[26] The segment of aorta that is affected varies: it may involve the aortic root, ascending aorta, descending thoracic, or abdominal aorta, and multiple aneurysms may occur. Aortic dilation is also noted to occur in association with CHD, either as a native phenomenon such as Tetralogy of Fallot and coarctation of aorta or following cardiac surgery such as Ross operation and arterial switch operation where the native pulmonary root is exposed to systemic arterial pressures.[26]

Echocardiographic surveillance of the aorta is an important aspect of the management of aortopathy and is typically performed at 6–12-month intervals. In order to ensure that measurements are reliable and reproducible, evaluation should include optimised two-dimensional imaging of all segments of the aorta to the extent possible as detailed previously (Fig 6a and b, Supplementary videos 6 and 7). This is of particular relevance in patients with this diagnosis, because decisions regarding pharmacological and/or surgical management are based on either absolute or temporal trends in the dimensions of the aorta. Standardised techniques for measurement and acquisition such as use of harmonics and lateral gain settings, use of the zoom feature to provide high-resolution images for obtaining measurements, and averaging measurements across three cardiac cycles resulted in high interobserver agreement (intraclass correlation coefficients of 0.92–0.99) in measurements.[27] Aortic valve function should be assessed, because aortic regurgitation can occur in aortopathy associated with bicuspid aortic valve, as well as with aortic dilation causing incomplete coaptation of the leaflets. The mitral and tricuspid valves must be examined in the apical and parasternal long-axis views for prolapse of single/multiple leaflets and resulting regurgitation – a common association with connective tissue disorders. The pulmonary root and main pulmonary artery should be imaged from the parasternal views to evaluate for dilation. Aortic dissection is rare in the paediatric age group but has been described.[28,29] Although transthoracic echocardiography is neither as sensitive nor as accurate as transoesophageal echocardiography, it may be helpful in diagnosing dissections in the aortic root and proximal ascending aorta. The diagnostic finding is an enlarged aorta with an intimal flap resulting in true and false lumens of the aorta (Fig 6c and d/ Supplementary videos 8 and 9). Additional findings include pericardial effusion or tamponade, aortic valve dysfunction, and ventricular dysfunction.[30]

Measuring vascular function of the aorta by echocardiography

The vascular biomechanics of the aorta including its elasticity and distensibility play an important role in the normal circulatory system. There is an increasing body of literature supporting the value of assessing the vascular function of the aorta. Echocardiography can be used to non-invasively measure the distensibility and stiffness of the aorta by factoring in the change in blood pressure and the dimensions of the ascending aorta by M-mode or two-dimensional echocardiography, during the cardiac cycle into calculations. These include the aortic distensibility index = [2(AoS – AoD)]/[AoD (SBP – DBP)],

https://doi.org/10.1017/S1047951116001219 Published online by Cambridge University Press

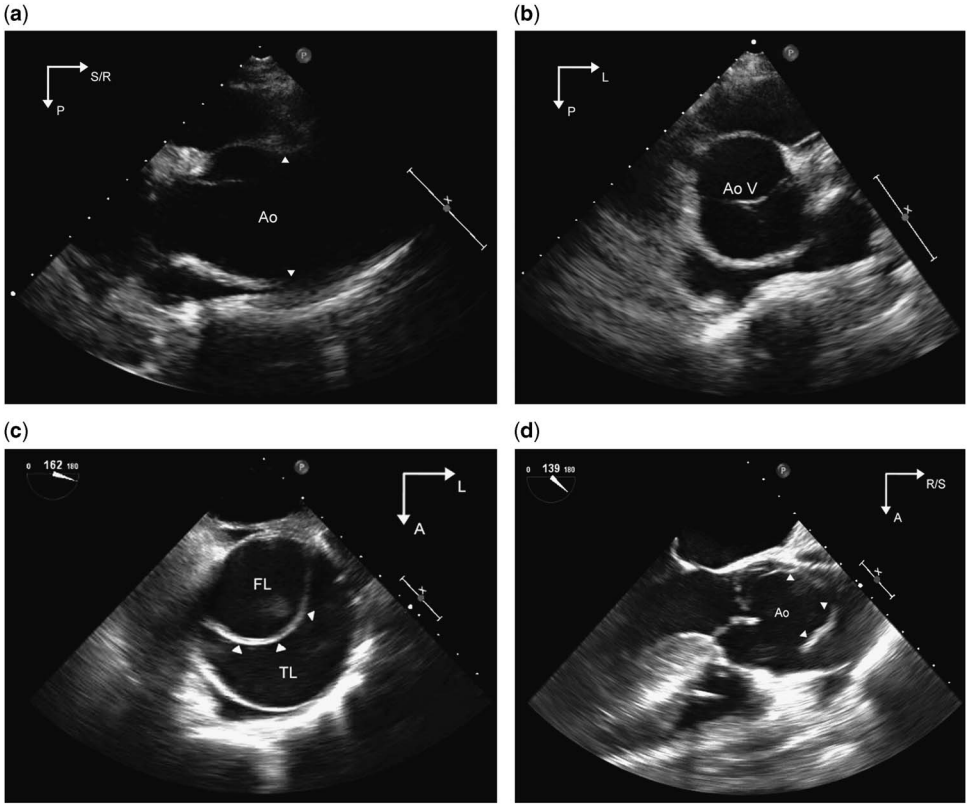

Figure 6.
*Panel (**a**)/Supplementary video 6 and Panel (**b**)/Supplementary video 7 are parasternal long- and short-axis images, respectively, demonstrating an enlarged aortic root and ascending aorta in a patient with Loeys–Dietz syndrome. The arrowheads point to the effacement of the sinotubular junction of the aorta that occurs with the enlargement of the ascending aorta. The aortic valve is trileaflet and appears normal. Panel (**c**)/Supplementary video 8 is a transoesophageal echocardiographic image of the cross-section of the ascending aorta in an adult patient with bicuspid aortic valve and aortic dissection. An intimal flap (arrowheads) is noted within the circular lumen of the aorta, separating it into true and false lumens. Panel (**d**)/Supplementary video 9 is a transoesophageal long-axis image of the aortic root showing the supero-inferior extent of the flap. Images are courtesy of Rigo Ramirez, MD, Mid America Heart Institute, Kansas City, Missouri, United States of America. Ao = aorta; AoV = aortic valve; A = anterior; FL= false lumen; L = left; P = posterior; R = right; S = superior; TL= true lumen.*

aortic stiffness index = ln (SBP/DBP)/[(AoS – AoD)/AoD], and Young's elastic modulus = SBP – DBP/[(AoS – AoD)/AoD], where AoS is the maximal dimension in systole, AoD the maximal dimension in diastole, and SBP and DBP systolic and diastolic blood pressures, respectively. The aortic distensibility index has been shown to be reduced in children with bicuspid aortic valve independent of the degree of aortic dilation, in coarctation of the aorta both before and after surgical repair, and after the arterial switch operation, suggesting that the aortic wall is intrinsically abnormal in these conditions.[31–34] Similar findings have been reported from the Marfan study sponsored by the Pediatric Heart Network, which revealed that increased aortic stiffness predicted dissection, increased rate of aortic dilation, and decreased response to β blockers (Lacro et al., abstract presented at American Heart Association scientific sessions, November 2015, unpublished). These studies indicate that there is prognostic value to studying the mechanics of the aortic wall in addition to structural assessment alone.

Newer modalities such as tissue Doppler and speckle tracking technology can also be used to quantify aortic strain, which is an additional measure of the compliance of the aorta.[35–37] Vitarelli et al[35] in their study of Marfan patients showed that increased aortic stiffness and reduced strain were useful in predicting dissection.

Multimodality imaging of the aorta

As described in the previous section, optimal imaging of the aorta by transthoracic echocardiography is challenging, especially in patients of larger size or those with difficult acoustic windows. The descending thoracic aorta is often incompletely and suboptimally imaged by transthoracic echocardiography. Transoesophageal echocardiography renders high-quality images of most segments of the aorta.

https://doi.org/10.1017/S1047951116001219 Published online by Cambridge University Press

With the current multiplane transducer technology, the ultrasound beam can be rotated in an arc of 180°, allowing for imaging the aorta in multiple planes. The distal ascending aorta and aortic arch are, however, difficult to visualise because of interposition of the airway. With transthoracic echocardiography, measurements of the aortic root and ascending aorta are typically made in the antero-posterior plane alone. Therefore, the dimensions can be underestimated if there is asymmetric enlargement of the aorta in the lateral plane. Similarly, insonation of the ascending aorta in an oblique plane can result in spuriously increased measurements. These limitations are overcome by modalities such as CT and MRI, which are more accurate and reproducible; they are therefore used as an adjunct to echocardiography in imaging the aorta.[38,39]

CT aortography is an excellent imaging modality for both acute and chronic conditions of the aorta and is the recommended first-line imaging modality for adults with acute aortic syndromes.[40] It is more widely available when compared with magnetic resonance angiography and acquisition times are only a few seconds; both modalities offer excellent spatial resolution and all segments of the aorta, including the branches, are adequately visualised. Both allow for excellent visualisation of the surrounding non-vascular structures and generation of three-dimensional reconstructions of the aorta. The main drawbacks of CT are the exposure to ionised radiation and iodinated contrast agents. MRI on the other hand is more time consuming and often requires breath holding, which limits its use without sedation in the paediatric age group. MRI is versatile in that it can be used to gain information about the physiology of the aorta, such as its compliance and stiffness, and to estimate aortic wall shear stress. CT may be the preferred technique in critically ill patients and in those with pacemakers/defibrillators, whereas MRI may be the modality of choice for stable, especially younger, patients for periodic surveillance.[40]

In summary, a variety of imaging modalities are available to the clinician for evaluation of the aorta – availability, cost, risk-to-benefit ratio, and the additive diagnostic value are all factors to be taken into consideration in determining the ideal technique for a given patient.

Conclusion

Echocardiography is an important tool in the assessment of the structure and function of the aorta, and is the primary imaging modality in the diagnosis of conditions such as supravalvar stenosis and the much rarer sinus of Valsalva aneurysm and aortoventricular tunnel. With attention to technique of image acquistion and measurement, assessment of the dimensions of the aorta can be made with high reliablity and reproducibility. Therefore, individual laboratories should follow standardised protocols. Nevertheless, the innate anatomical features of the aorta can make visualisation of some of its sections by echocardiography challenging; CT and MRI are superior in this regard. Finally, it is possible to assess the vascular mechanics of the aorta by echocardiography; the clinical relevance of such parameters is uncertain, but offers promise.

Acknowledgements

None.

Financial Support

This research received no specific grant from any funding agency, commercial, or not-for-profit sectors.

Conflicts of Interest

None.

Ethical Standards

The authors assert that all procedures contributing to this study comply with the ethical standards of the relevant national guidelines on human experimentation and with the Helsinki Declaration of 1975, as revised in 2008.

Supplementary material

To view supplementary material for this article, please visit http://dx.doi.org/10.1017/S1047951116001219

References

1. Goldstein SA, Evangelista A, Abbara S, et al. Multimodality imaging of diseases of the thoracic aorta in adults: from the American Society of Echocardiography and the European Association of Cardiovascular Imaging: endorsed by the Society of Cardiovascular Computed Tomography and Society for Cardiovascular Magnetic Resonance. J Am Soc Echocardiogr 2015; 28: 119–182.
2. Lopez L, Colan SD, Frommelt PC, et al. Recommendations for quantification methods during the performance of a pediatric echocardiogram: a report from the Pediatric Measurements Writing Group of the American Society of Echocardiography Pediatric and Congenital Heart Disease Council. J Am Soc Echocardiogr 2010; 23: 465–495.
3. Pettersen MD, Du W, Skeens ME, Humes RA. Regression equations for calculation of z scores of cardiac structures in a large cohort of healthy infants, children, and adolescents: an echocardiographic study. J Am Soc Echocardiogr 2008; 21: 922–934.
4. Sluysmans T, Colan SD. Theoretical and empirical derivation of cardiovascular allometric relationships in children. J Appl Physiol 2005; 99: 445–457.
5. Kharwar RB, Narain VS, Sethi R. Real time three-dimensional transthoracic echocardiography of ruptured left sinus of Valsalva aneurysm to left ventricle. Echocardiography 2013; 30: E331–E335.

6. Vijay SK, Narain VS, Sethi R, Chandra S, Puri A. Live three-dimensional transthoracic echocardiography of giant aorto-right ventricular tunnel. Eur Heart J Cardiovasc Imaging 2013; 14: 86.
7. Chang CY, Hsiung MC, Tsai SK, et al. Live three-dimensional transesophageal echocardiography in an unusual case of aorto-left ventricular tunnel with a large interventricular septal aneurysm. Echocardiography 2011; 28: E12–E15.
8. Merla G, Brunetti-Pierri N, Piccolo P, Micale L, Loviglio MN. Supravalvular aortic stenosis: elastin arteriopathy. Circ Cardiovasc Genet 2012; 5: 692–696.
9. Stamm C, Friehs I, Ho SY, Moran AM, Jonas RA, del Nido PJ. Congenital supravalvar aortic stenosis: a simple lesion? Eur J Cardiothorac Surg 2001; 19: 195–202.
10. Dayan J, Sett S, Krishnan U. Silent rupture of sinus of Valsalva aneurysm: a refutation of the Okham's razor principle. Cardiol Young 2011; 21: 713–715.
11. Math RS, Saxena A, Chakraborty P, Reddy SM, Bisoi A. An unusual case of dissecting aneurysms involving both coronary sinuses of Valsalva. J Am Soc Echocardiogr 2010; 23: 457–459 458 e.
12. Lahrouchi N, Rammeloo LA, Koolbergen DR, Hruda J. Ruptured aneurysm of the right coronary sinus of Valsalva in a child with down syndrome. Cardiol Young 2014; 24: 376–378.
13. Vijayalakshmi IB, Devananda NS, Chitra N. A patient with aneurysms of both aortic coronary sinuses of Valsalva obstructing both ventricular outflow tracts. Cardiol Young 2009; 19: 537–539.
14. Cheng TO, Yang YL, Xie MX, et al. Echocardiographic diagnosis of sinus of Valsalva aneurysm: a 17-year (1995–2012) experience of 212 surgically treated patients from one single medical center in China. Int J Cardiol 2014; 173: 33–39.
15. Mithani AA, Polimenakos AC, Santucci BA. Ruptured sinus of Valsalva found incidentally in a patient with Tetralogy of Fallot. Pediatr Cardiol 2013; 34: 1914–1917.
16. Nakamura Y, Aoki M, Hagino I, Koshiyama H, Fujiwara T, Nakajima H. Case of congenital aneurysm of sinus of Valsalva with common arterial trunk. Ann Thorac Surg 2014; 97: 710–712.
17. Thankavel PP, Lemler MS, Ramaciotti C. Unruptured sinus of valsalva aneurysm in a neonate with hypoplastic left heart syndrome: echocardiographic diagnosis and features. Echocardiography 2014; 31: E85–E87.
18. McKay R. Aorto-ventricular tunnel. Orphanet J Rare Dis 2007; 2: 41.
19. Mahle WT, Kreeger J, Silverman NH. Echocardiography of the aortopulmonary window, aorto-ventricular tunnels, and aneurysm of the sinuses of Valsalva. Cardiol Young 2010; 20 (Suppl 3): 100–106.
20. Deshpande SR, Fyfe DA. Aorto-right atrial tunnel: fetal heart failure, diagnosis, and treatment. Pediatr Cardiol 2010; 31: 299–300.
21. Vida VL, Bottio T, Stellin G. An unusual case of aorto-left ventricular tunnel. Cardiol Young 2004; 14: 203–205.
22. Singh SK, Dwivedi SK, Kumar A, et al. Aneurysmal aorto-right ventricular tunnel. Ann Thorac Surg 2012; 93: e21–e22.
23. Ziesenitz VC, Gorenflo M, Loukanov T. Repair of an aorto-right ventricular tunnel in a newborn. Cardiol Young 2016; 26: 147–148.
24. Jureidini SB, de Mello D, Nouri S, Kanter K. Aortico-right ventricular tunnel and critical pulmonary stenosis: diagnosis by two-dimensional and Doppler echocardiography and angiography. Pediatr Cardiol 1989; 10: 99–103.
25. Hruda J, Hazekamp MG, Sobotka-Plojhar MA, Ottenkamp J. Repair of aorto-right ventricular tunnel with pulmonary stenosis and an anomalous origin of the left coronary artery. Eur J Cardiothorac Surg 2002; 21: 1123–1125.
26. Francois K. Aortopathy associated with congenital heart disease: a current literature review. Ann Pediatr Cardiol 2015; 8: 25–36.
27. Selamet Tierney ES, Levine JC, Chen S, et al. Echocardiographic methods, quality review, and measurement accuracy in a randomized multicenter clinical trial of Marfan syndrome. J Am Soc Echocardiogr 2013; 26: 657–666.
28. Carlson M, Airhart N, Lopez L, Silberbach M. Moderate aortic enlargement and bicuspid aortic valve are associated with aortic dissection in Turner syndrome: report of the international turner syndrome aortic dissection registry. Circulation 2012; 126: 2220–2226.
29. Fikar CR. Acute aortic dissection in children and adolescents: diagnostic and after-event follow-up obligation to the patient and family. Clin Cardiol 2006; 29: 383–386.
30. Baliga RR, Nienaber CA, Bossone E, et al. The role of imaging in aortic dissection and related syndromes. JACC Cardiovasc Imaging 2014; 7: 406–424.
31. Oulego-Erroz I, Alonso-Quintela P, Mora-Matilla M, Gautreaux Minaya S, Lapena-Lopez de Armentia S. Ascending aorta elasticity in children with isolated bicuspid aortic valve. Int J Cardiol 2013; 168: 1143–1146.
32. Pees C, Michel-Behnke I. Morphology of the bicuspid aortic valve and elasticity of the adjacent aorta in children. Am J Cardiol 2012; 110: 1354–1360.
33. Vogt M, Kuhn A, Baumgartner D, et al. Impaired elastic properties of the ascending aorta in newborns before and early after successful coarctation repair: proof of a systemic vascular disease of the prestenotic arteries? Circulation 2005; 111: 3269–3273.
34. Chen RH, Wong SJ, Wong WH, Cheung YF. Arterial mechanics at rest and during exercise in adolescents and young adults after arterial switch operation for complete transposition of the great arteries. Am J Cardiol 2014; 113: 713–718.
35. Vitarelli A, Conde Y, Cimino E, et al. Aortic wall mechanics in the Marfan syndrome assessed by transesophageal tissue Doppler echocardiography. Am J Cardiol 2006; 97: 571–577.
36. Vitarelli A, Conde Y, Cimino E, et al. Assessment of ascending aorta distensibility after successful coarctation repair by strain Doppler echocardiography. J Am Soc Echocardiogr 2008; 21: 729–736.
37. Teixeira R, Moreira N, Baptista R, et al. Circumferential ascending aortic strain and aortic stenosis. Eur Heart J Cardiovasc Imaging 2013; 14: 631–641.
38. Nejatian A, Yu J, Geva T, White MT, Prakash A. Aortic measurements in patients with aortopathy are larger and more reproducible by cardiac magnetic resonance compared with echocardiography. Pediatr Cardiol 2015; 36: 1761–1773.
39. van der Linde D, Rossi A, Yap SC, et al. Ascending aortic diameters in congenital aortic stenosis: cardiac magnetic resonance versus transthoracic echocardiography. Echocardiography 2013; 30: 497–504.
40. Goldstein SA, Evangelista A, Abbara S, et al. Multimodality imaging of diseases of the aorta in adults. J Am Soc Echocardiogr 2015; 28: 119–182.